

See discussions, stats, and author profiles for this publication at: <https://www.researchgate.net/publication/277602224>

# Electrochemical Water Splitting Based on Hypochlorite Oxidation

ARTICLE in JOURNAL OF THE AMERICAN CHEMICAL SOCIETY · JUNE 2015

Impact Factor: 12.11 · DOI: 10.1021/jacs.5b02087 · Source: PubMed

---

READS

35

4 AUTHORS, INCLUDING:



**Elisabet Ahlberg**

University of Gothenburg

149 PUBLICATIONS 2,126 CITATIONS

SEE PROFILE



**Petr Krtil**

Academy of Sciences of the Czech Republic

77 PUBLICATIONS 1,184 CITATIONS

SEE PROFILE

# Electrochemical Water-Splitting Based on Hypochlorite Oxidation

Kateřina Minhov Macounov,<sup>†</sup> Nina Simic,<sup>§</sup> Elisabet Ahlberg,<sup>\*,‡</sup> and Petr Krtil<sup>\*,†</sup>

<sup>†</sup>J. Heyrovsk Institute of Physical Chemistry, Academy of Sciences of the Czech Republic, Doleřskova 3, 18223 Prague, Czech Republic

<sup>‡</sup>Department of Chemistry and Molecular Biology, University Gothenburg, SE-41296 Gothenburg, Sweden

<sup>§</sup>AkzoNobel Pulp and Performance Chemicals, SE-445 80 Bohus, Sweden

## S Supporting Information

**ABSTRACT:** Effective catalytic water-splitting can be electrochemically triggered in an alkaline solution of sodium hypochlorite. Hypochlorite oxidation on polycrystalline platinum yields ClO• radicals, which initiate a radical-assisted water-splitting, yielding oxygen, hydrogen peroxide, and protons. The efficiency of the O<sub>2</sub> production corresponds to about two electrons per molecule of the produced O<sub>2</sub> and is controlled primarily by the hypochlorite concentration and pH.

Oxidation of water is one of the most challenging tasks of modern electrochemistry, mainly in connection with the utilization of renewable energy sources based on wind or solar power.<sup>1</sup> This so-called hydrogen economy concept is based on (photo)electrochemical water-splitting to hydrogen and oxygen to store the renewable electricity. The stored energy can be converted back into electricity in a fuel cell. The hydrogen economy cycle is, in fact, controlled by the oxygen evolution/reduction process, which represents the limiting process, mainly due to significant kinetic hindrance of the charge-transfer reaction. Oxygen evolution, both heterogeneous<sup>2–5</sup> and homogeneous,<sup>6–10</sup> has consequently attracted significant theoretical attention.<sup>11–14</sup> Regardless of the mode of operation, it is assumed that the water-oxidizing catalyst enters a catalytic cycle in which it gets activated either by an external electric field (e.g., holes generated in a photocathode) or by the so-called primary oxidant.<sup>15</sup> These primary oxidants are based on Ce<sup>4+</sup>/Ce<sup>3+</sup> redox couple,<sup>16</sup> peroxosulfates,<sup>17,18</sup> or periodate.<sup>19</sup> Despite significant driving force, the primary oxidants do not oxidize water due to slow kinetics. Instead, the primary oxidants participate in water oxidation<sup>20</sup> in the presence of additional water oxidation catalyst, most likely via a radical mechanism.<sup>20</sup> However, their actual role has not been outlined in depth. The majority of the so-far reported primary oxidants are confined to acid media, with the exception of hypochlorite, which has been used in several studies in alkaline media.<sup>15,21,22</sup> Oxygen production has been reported to accompany the anodic oxidation of hypochlorite,<sup>23,24</sup> but the process has never been studied in connection with the oxygen evolution. The suitability of hypochlorite as a primary oxidant in water oxidation studies has been questioned on the grounds of the rapid exchange of oxygen between water and hypochlorite anion, preventing the conclusive proof of water oxidation.<sup>23,25</sup> Exploration of hypochlorite as the primary oxidant was also discouraged by its significantly worse activity compared with, e.g.,

oxone.<sup>22</sup> Hypochlorite involvement has also been suggested to explain the photocatalytic water-splitting on illuminated AgCl.<sup>26,27</sup> The details of the process, however, have never been elucidated.

The observed behavior can be qualified realizing that the hypochlorite—in contrast to the other primary oxidants—does not feature the redox-active atom in the highest attainable stable oxidation state. As a result, hypochlorite offers more complex and abundant redox chemistry; it can be oxidized and act as an efficient water-splitting catalyst itself. We report here, for the first time, efficient water oxidation triggered by electrochemical oxidation of hypochlorite, in which the hypochlorite anion can act as a catalyst in a relatively broad range of experimental conditions. We combine the results of linear sweep voltammetry with differential electrochemical mass spectrometry (DEMS) to address the mechanism of the hypochlorite-catalyzed water-splitting and to quantify its efficiency.

The hypochlorite samples were prepared by letting chlorine gas into a 5 M NaOH solution (Scharlau, reagent grade, ACS, ISO, Reag.Ph Eur) until a hypochlorite concentration of 1.6 M was reached. The solution was chilled and was stored in the dark and cool. The hypochlorite stock solution contained an equimolar amount of sodium chloride. Hypochlorite oxidation was studied in 0.1 M NaClO<sub>4</sub> (Aldrich, p.a.) solutions containing variable amounts of hypochlorite. All solutions were prepared using Milli-Q-quality water; the more concentrated hypochlorite solutions (*c* > 0.05 M) were studied under native pH. In the case of more diluted solution, the pH was adjusted to 9.5 by adding a few drops of 0.1 M NaOH (Aldrich, ACS grade). The water oxidation experiments were performed in a three-electrode arrangement using a single-compartment Kel-F cell adjusted for simultaneous use of the online mass spectra in the DEMS mode. Oxidation of the hypochlorite was performed by linear scan voltammetry at a polarization rate of 5 mV/s using a Pt mesh (electrode area 0.4 cm<sup>2</sup>, open area 60%) working electrode, Pt auxiliary, and Ag/AgCl reference electrode. The measured potentials were recalculated and are quoted in reversible hydrogen electrode (RHE) scale to allow for unhindered comparison. The DEMS apparatus consisted of a Prisma QMS200 quadrupole mass spectrometer (Balzers) connected to a TSU071 turbomolecular drag pumping station (Balzers).

The hypochlorite is electrochemically oxidized at potentials positive to 1.2 V vs RHE (see Figure 1A). This anodic process is

Received: February 26, 2015

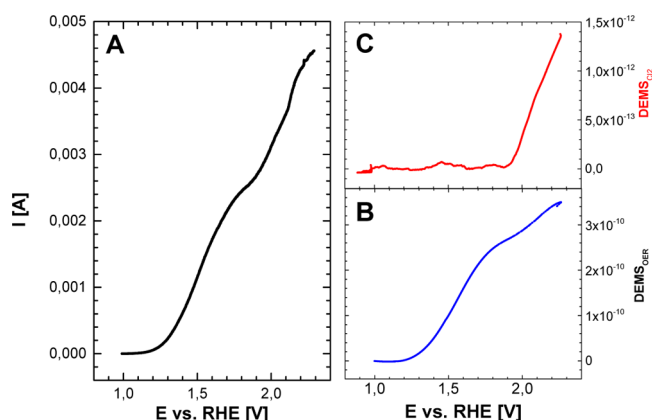


**Figure 1.** (A) Linear sweep voltammogram along with DEMS-based signals corresponding to oxygen evolution (B) and chlorine evolution (C), reflecting the hypochlorite oxidation on polycrystalline Pt electrode. The data were recorded in solution containing 0.05 M NaClO in 0.1 M NaClO<sub>4</sub> at pH 9.5. The data were recorded at polarization rate 5 mV/s.

immediately accompanied by evolution of O<sub>2</sub>, which is detected in the simultaneously recorded mass spectrometric signal (see Figure 1B). O<sub>2</sub> apparently represents the only detectable product at potentials below 1.9 V vs RHE when small amounts of chlorine ( $m/z = 70, 35, 37$ , and  $74$ ) and hydrochloric acid ( $m/z = 36$ ) are also detected (see Figure 1C). The observed chlorine evolution can be attributed to oxidation of chloride ions. The DEMS detection of chlorine is allowed by the apparent decrease of the surface pH during O<sub>2</sub> evolution, preventing immediate hydrolysis of the produced chlorine. The detected hydrochloric acid ( $m/z$  of 36) is probably formed in the ionization part of the DEMS apparatus rather than directly in the liquid phase, given the fact that the gas phase leaving the DEMS cell contains, aside from the electrochemically generated chlorine, also excess water. It needs to be noted that both oxygen and chlorine are detected at potentials positive to the corresponding pH-adjusted standard potentials (1.23 V for oxygen evolution and 1.91 V for chlorine evolution).

Quantification of the extent of O<sub>2</sub> production as well as its origin is summarized in Figures 2 and 3. The amount of detected O<sub>2</sub> can be determined on the basis of calibration of the DEMS setup using oxygen evolution in chloride- and hypochlorite-free solution (see Figure 1S in the Supporting Information). Using the calibration shown in Figure 1S, we can express the extent of evolved O<sub>2</sub> in terms of  $z$ , which represents the apparent number of electrons entering the external circuit at the anode during evolution of one molecule of O<sub>2</sub>. The potential and concentration dependence of  $z$  is summarized in Figure 2.

In contrast to the expectation, the amount of the evolved O<sub>2</sub> significantly exceeds that one intuitively anticipates for a parasitic electrode reaction. While the conventional electrochemical O<sub>2</sub> evolution assumes a transfer of four electrons from water to the anode (to evolve one molecule of O<sub>2</sub>), comparison of the anodic charge with the amount of detected O<sub>2</sub> consistently yields  $z$  values smaller than 4. The apparent number of electrons needed to evolve O<sub>2</sub> is lower at less positive potentials and decreases with decreasing hypochlorite concentration. The  $z$  value also apparently increases with increasing extent of electrolysis, as can be seen from the dependence of  $z$  on the passed charge (see panel B of Figure 2).  $z$  values smaller than 4 indicate that the O<sub>2</sub> evolution mechanism involves homogeneous reaction(s). Both trends reflected in Figure 2 also suggest the role of the pH, which

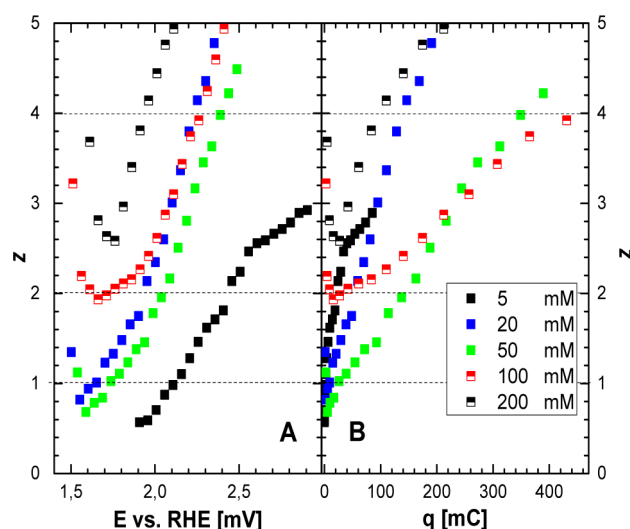


**Figure 2.** Apparent numbers of electrons needed to evolve one molecule of O<sub>2</sub> as a function of the electrode potential (A) and of the passed charge (B). Data were extracted from DEMS experiments carried out in 0.1 M NaClO<sub>4</sub> containing variable amounts of hypochlorite. The actual hypochlorite concentrations are shown in the inset. The experimental details are the same as in Figure 1. The dashed lines, marking different charge efficiency of the water oxidation, were added to guide the eye.

increases with increasing hypochlorite concentration and decreases with increasing extent of the oxidation process.

The data in Figure 2 show that O<sub>2</sub> evolution is significantly favored in diluted solutions, suggesting a radical nature of the O<sub>2</sub> evolution process. It needs to be stressed that the detection of gaseous O<sub>2</sub> does not constitute evidence of water oxidation since the oxygen can, in principle be released from the hypochlorite anion via decomposition of the ClO<sup>•</sup> radical.<sup>28</sup>

Water oxidation is conclusively confirmed by the detection of hydrogen peroxide, the formation of which is reflected in the time course of the DEMS signal with  $m/z = 34$ , observed in experiments featuring an initial hypochlorite concentration of 0.005 M and higher. Hydrogen peroxide (H<sub>2</sub>O<sub>2</sub>) is formed in the homogeneous phase and can be detected only if contact with the Pt electrode is avoided. Its detection is, therefore, facilitated by the large open area of the Pt working mesh electrode. It may be envisaged that its contact with the Pt electrode leads to oxidation, producing water and oxygen, which does not affect the  $z$ . The apparent lack of the H<sub>2</sub>O<sub>2</sub> signal in experiments with hypochlorite concentration lower than 0.005 M can be attributed to a low sensitivity of the DEMS approach to H<sub>2</sub>O<sub>2</sub> due to the low volatility of H<sub>2</sub>O<sub>2</sub> in aqueous solutions. The H<sub>2</sub>O<sub>2</sub> signal tracks that of the evolved O<sub>2</sub>, and its relative abundance decreases with electrode potential (see Figure 3). The molar ratio of H<sub>2</sub>O<sub>2</sub> and O<sub>2</sub> decreases with increasing hypochlorite concentration (see Figure 3C). The overall efficiency of the hypochlorite-triggered oxygen evolution decreases with increasing hypochlorite concentration (see Figure 2). This also shows the concentration dependence of the amount of evolved O<sub>2</sub>, which initially increases with hypochlorite concentration but reaches a limiting value at a concentration of 0.05 M (see Figure 2S in the Supporting Information).

The apparent disagreement between the detected amount of O<sub>2</sub> and recorded charge in fact does not violate the known stoichiometry of the O<sub>2</sub> and H<sub>2</sub>O<sub>2</sub> formation, which require the transfer of four and two electrons, respectively. The observed behavior indicates that only a fraction of the charge needed to

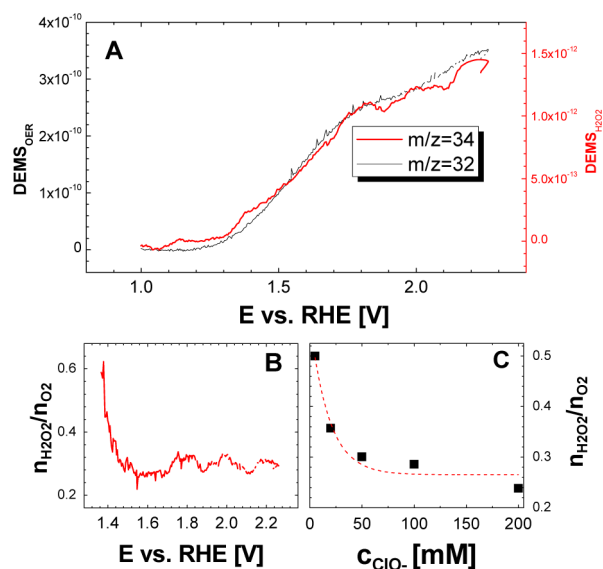
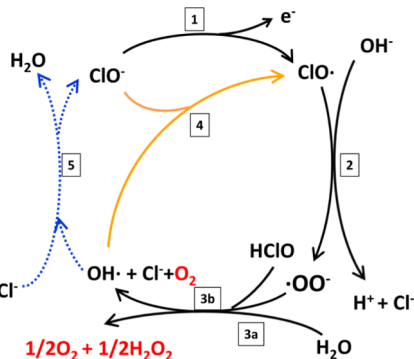


**Figure 3.** (A) DEMS signals corresponding to  $O_2$  and  $H_2O_2$  formed during hypochlorite oxidation, and plots of the potential (B) and concentration (C) dependences of the ratio between formed  $H_2O_2$  and  $O_2$ . The results were extracted from voltammetric data. Experimental conditions were identical to those in Figure 1. The signal of  $m/z = 34$  was smoothed with a FFT filter (cutoff frequency 0.02 Hz).

produce  $O_2$  is transported through the external circuit to the counter electrode, and the majority of the transferred electrons has to be accommodated by the products of the hypochlorite oxidation. The hypochlorite oxidation products need, therefore, accommodate up to three electrons per  $O_2$  molecule. Given the fact that the whole process is electrochemically triggered, one may use the combination of  $z$  and the presence of  $H_2O_2$  to outline the likely mechanism of the processes accompanying the hypochlorite oxidation.

The hypochlorite oxidation process is known to start by a single-electron oxidation, producing the  $ClO^\bullet$  radical (reaction (1) in Scheme 1).<sup>24</sup> Formation of the  $ClO^\bullet$  radical initiates a complex reaction sequence in which the system can follow different reaction pathways. The  $ClO^\bullet$  radical reacts with water to form the superoxide radical anion (reaction (2) in Scheme 1).

#### Scheme 1. Reaction Pathways of the Hypochlorite Oxidation in 0.1 M $NaClO_4$ Medium<sup>a</sup>



<sup>a</sup>Detected reaction products are marked in red. The dotted arrows represent processes without definite stoichiometry. Orange and blue arrows code the reaction steps distinguishing reaction mechanisms A (radical chain) and B (catalytic one); black arrows mark processes common to both reaction mechanisms.

The formed superoxide radical anion may enter numerous chemical reactions, yielding water,  $O_2$ ,  $H_2O_2$ , and  $OH^\bullet$  radicals (see Supporting Information for detailed analysis). The superoxide radical anion is known to disproportionate to  $O_2$  and  $H_2O_2$ <sup>29</sup> (reaction (3a) in Scheme 1). The presence of  $H_2O_2$  apparently conforms to this reaction, particularly at low hypochlorite concentrations (see Figure 3C). The  $O_2$  formation via superoxide anion radical decomposition, however, requires a transfer of at least two electrons across the electrode–electrolyte interface to produce an  $O_2$  molecule, which contradicts the observed values of  $z$ .

The superoxide anion radical may alternatively react with various chloro-containing species, as outlined in ref 29. The only process proceeding at an appreciable rate represents its reaction with hypochlorous acid, producing  $O_2$  and  $OH^\bullet$  radical (reaction (3b) in Scheme 1).<sup>29</sup> The hypochlorous acid is in equilibrium with present hypochlorite; its concentration (and the whole reaction (3b)) is controlled by the pH and henceforth changes with overall hypochlorite concentration as well as with the extent of oxidation. The  $O_2$  produced in step (3b) should yield  $z = 1$ , as it is observed in experiments at low potentials. The presence of both  $O_2$  and  $H_2O_2$  among the reaction products, however, indicates that both reactions steps (3a) and (3b) proceed simultaneously, and their ratio is primarily controlled by the pH in the electrode's vicinity. Regardless of the actual mechanism of the  $OO^{\bullet-}$  decomposition, the reaction sequence (1)–(3) is connected with hypochlorite depletion and chloride accumulation.

A comparison of the chloride content before and after hypochlorite oxidation experiment, however, does not support the chloride accumulation in the system (see Figure 4). Data

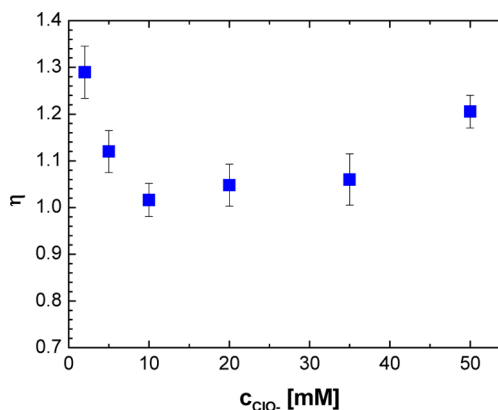


**Figure 4.** Ratio between chloride concentration before and after water oxidation experiment as a function of the hypochlorite concentration. The hypochlorite solutions were subject to the same experimental conditions as in Figure 1. The chloride concentrations were determined by gravimetric titration with  $AgNO_3$ .

presented in Figure 4 clearly show the system's enrichment with chloride in experiments with the lowest hypochlorite concentrations ( $c < 0.01$  M). In experiments where the concentration of hypochlorite ranged between 0.01 and 0.05 M, the hypochlorite-triggered water oxidation causes just a minor increase of the chloride content. This behavior reflects a complex nature of the process indicating that the produced radical species react further.

The formed  $OH^\bullet$  radicals are highly oxidizing agents<sup>30</sup> and may react either with hypochlorite anion (reaction mechanism A, marked orange in Scheme 1) or with chlorides (reaction mechanism B, marked blue in Scheme 1). Reaction mechanism A



produces  $\text{ClO}^\bullet$  radicals that re-enter the reaction step (2). Reaction mechanism B regenerates the hypochlorite anion, which may re-enter the oxidation process in reaction (1). Reaction mechanism B in fact closes a catalytic cycle in which the hypochlorite acts effectively as a water oxidation catalyst. It ought to be stressed that the formation of  $\text{ClO}^-$  in step (5) is a process of complex nature involving several reaction steps, as shown in refs 31 and 32. It also does not include possible involvement of the surface, which is less likely in our experiments due to the large open area of the electrode. As a result, we include this process in Scheme 1 only in its summary form. Detailed analysis of process (5) is given in the Supporting Information.

The overall process includes two reaction mechanisms. Reaction mechanism A displays the features of a chain-like propagation reaction, so the apparent number of electrons  $z$  needed to evolve  $\text{O}_2$  decreases with the turnover number and may drop below 1. The apparent number of electrons  $z$  needed to evolve  $\text{O}_2$  in reaction mechanism B ranges between 1 and 2, depending on the contribution from reactions (3a) and (3b). Reaction mechanisms A and B may proceed simultaneously or exclusively. The apparent potential-dependent shift from the radical chain reaction mechanism A to the catalytic reaction mechanism B is most likely pH-triggered.

Despite the intrinsic poor stability of Pt in anodic processes in the presence of chlorides,<sup>33</sup> both reaction mechanisms A and B proposed for the hypochlorite oxidation-triggered  $\text{O}_2$  evolution processes are rather potent in water oxidation. Their potential for technological exploration is, however, significantly different, bearing in mind that the purpose of water oxidation is not to generate  $\text{O}_2$  but to compensate (and enable) the desirable electrocatalytic  $\text{H}_2$  evolution. The hypochlorite-based process significantly facilitates the kinetics of the heterogeneous charge transfer, changing the four-electron charge transfer into a single-electron transfer. On the other hand, the fact that both reaction mechanisms evolve  $\text{O}_2$  primarily in homogeneous reactions breaks the conventional relationship between the amount of evolved  $\text{O}_2$  and charge “enabled” for the cathodic production of  $\text{H}_2$ . The radical chain nature of reaction mechanism A then becomes ultimately unsuitable for its application in renewable energy storage, despite its extremely favorable efficiency in oxidative water-splitting, and it needs to be suppressed in practical applications. Catalytic reaction mechanism B, on the other hand, retains the potential to be a viable alternative in the water (photo)electrolysis, namely if combined as a co-catalyst with durable and active oxide-based anode material(s). The overall feasibility of the process may be further improved by optimizing the electrode material and geometry.

## ■ ASSOCIATED CONTENT

### ■ Supporting Information

Calibration graphs for the DEMS quantification and summary of the amounts of evolved  $\text{O}_2$  and chlorine. The Supporting Information is available free of charge on the ACS Publications website at DOI: 10.1021/jacs.5b02087.

## ■ AUTHOR INFORMATION

### Corresponding Authors

\*ela@chem.gu.se

\*petr.krttil@jh-inst.cas.cz

### Notes

The authors declare no competing financial interest.

## ■ ACKNOWLEDGMENTS

Financial support from the Swedish Energy Agency (Project 33280-1) and the Swedish Research Council (Project 621-2010-4035) is gratefully acknowledged.

## ■ REFERENCES

- (1) Lewis, N. S.; Nocera, D. *Proc. Natl. Acad. Sci. U.S.A.* **2006**, *104*, 15729.
- (2) Kanan, M. W.; Nocera, D. G. *Science* **2008**, *321*, 1072.
- (3) Suntivich, J.; May, K. J.; Gasteiger, H. A.; Goodenough, J. B.; Shao-Horn, Y. *Science* **2011**, *334*, 1383.
- (4) Trasatti, S. *Electrochim. Acta* **2000**, *45*, 2377.
- (5) Fierro, S.; Nagel, T.; Baltruschat, H.; Comninellis, Ch. *Electrochem. Commun.* **2007**, *45*, 2377.
- (6) Gersten, S. W.; Samules, G. J.; Meyer, T. J. *J. Am. Chem. Soc.* **1982**, *104*, 4029.
- (7) Concepcion, J. J.; Jurss, J. W.; Templeton, J. L.; Mayer, T. J. *Proc. Natl. Acad. Sci. U.S.A.* **2008**, *105*, 17632.
- (8) Zhong, R.; Thummel, R. P. *J. Am. Chem. Soc.* **2005**, *127*, 12802.
- (9) Kunkely, H.; Vogler, A. *Angew. Chem., Int. Ed* **2009**, *48*, 1685.
- (10) McEvoy, J. P.; Brudvig, G. W. *Chem. Rev.* **2006**, *106*, 4455.
- (11) Rossmeisl, J.; Qu, Z. W.; Zhu, H.; Kroes, G. J.; Nørskov, J. K. *J. Electroanal. Chem.* **2007**, *607*, 83.
- (12) Koper, M. T. M. *J. Electroanal. Chem.* **2011**, *660*, 254.
- (13) Busch, M.; Ahlberg, E.; Panas, I. *Phys. Chem. Chem. Phys.* **2011**, *13*, 15069.
- (14) Halck, N. B.; Petrykin, V.; Krttil, P.; Rossmeisl, J. *Phys. Chem. Chem. Phys.* **2014**, *16*, 13682.
- (15) Parent, A. R.; Crabtree, R. H.; Brudvig, G. W. *Chem. Soc. Rev.* **2013**, *42*, 2247.
- (16) Gilbert, J. A.; Eggleston, D. S.; Murphy, W. R.; Geselowitz, D. A.; Gersten, S. W.; Hodgson, D. J.; Meyer, T. J. *J. Am. Chem. Soc.* **1985**, *107*, 3855.
- (17) Rotzinger, F. P.; Munavalli, S.; Comte, P.; Hurst, J. K.; Gratzel, M.; Pern, F. J.; Frank, A. J. *J. Am. Chem. Soc.* **1987**, *107*, 6619.
- (18) Robert, A.; Meunier, B. *New J. Chem.* **1988**, *12*, 885.
- (19) Parent, A. R.; Brewster, T. P.; DeWolf, W.; Crabtree, R. H.; Brudvig, G. W. *Inorg. Chem.* **2012**, *51*, 6147.
- (20) Beckmann, K.; Uchtenhage, H.; Berggren, G.; Anderlund, M. F.; Thapper, A.; Messinger, J.; Styring, S.; Kurz, Ph. *Energy Environ. Sci.* **2008**, *1*, 668.
- (21) Limburg, J.; Vrettos, J. S.; Liable-Sands, L. M.; Rheingold, A. L.; Crabtree, R. H.; Brudvig, G. W. *Science* **1999**, *283*, 1524.
- (22) Limburg, J.; Vrettos, J. S.; Chen, H.; de Paula, J. C.; Crabtree, R. H.; Brudvig, G. W. *J. Am. Chem. Soc.* **2001**, *123*, 423.
- (23) Foerster, F. Z. *Elektrochem.* **1902**, 515.
- (24) Spasojevic, M.; Krstajic, N.; Spasojevic, P.; Ribic-Zelenovic, L. *Chem. Eng. Res. Des.* **2015**, *93*, 591.
- (25) Meunier, B.; Guilmet, E.; De Carvalho, M.-E.; Poilblanc, R. *J. Am. Chem. Soc.* **2000**, *122*, 2675.
- (26) Lanz, M.; Schurch, D.; Calzaferri, G. *J. Photochem. Photobiol. A, Chem.* **1999**, *120*, 105.
- (27) Pfanner, K.; Gfeller, N.; Calzaferri, G. *J. Photochem. Photobiol. A, Chem.* **1996**, *95*, 175.
- (28) Molina, L. T.; Molina, M. J. *J. Phys. Chem.* **1987**, *91*, 433.
- (29) Behar, D.; Czapski, G.; Rabani, J.; Dorfman, L. M.; Schwarz, H. A. *J. Phys. Chem.* **1970**, *74*, 3209.
- (30) Buxton, G. V.; Greenstock, C. L.; Helman, W. P.; Ross, A. B. *J. Phys. Chem. Ref. Data* **1988**, *17*, 573.
- (31) Saran, M.; Beck-Speier, I.; Fellerhoff, B.; Bauer, G. *Free Radical Biol. Med.* **1999**, *26*, 482.
- (32) Jayson, G. G.; Parson, B. J.; Swallow, A. J. *J. Chem. Soc., Faraday Trans. 1* **1973**, *69*, 1597.
- (33) Wang, Z.; Tada, E.; Nishikata, A. *J. Electrochem. Soc.* **2014**, *161*, F845.